Babylonian Journal of Mechanical Engineering
Vol.2025, **pp**. 104–120
DOI: https://doi.org/10.58496/BJME/2025/008; ISSN: 3006-5410
https://mesopotamian.press/journals/index.php/BJME

Research Article

A numerical study of time-dependent Casson nanofluid flow with convection and Joule heating over a stretching surface

M. Nazim Tufail [1, *], Nadia Ayub [1], Y. Khan [2], S. Ilyas [3]

[1] *Department of Mathematics, University of Management and Technology Sialkot Campus, Pakistan.*
[2] *Department of Mathematics, University of Hafr Al Batin, Hafr Al Batin 31991, Saudi Arabia.*
[3] *Department of Zoology, University of Sialkot, Sialkot Punjab, Pakistan.*

ARTICLE INFO

Article History
Received 25 May 2025
Revised: 21 Jun 2025
Accepted 20 Jul 2025
Published 28 Aug 2025

Keywords
Casson nanofluid
mixed convection
Joule heating
Mass transfer
stretching surface
bvp4c method

ABSTRACT

This study focuses on the behavior of Casson nanofluid under mixed convection, Joule heating, and mass transfer effects over a stretching surface. The governing equations for the conservation of momentum, mass, energy, and species transfer are simplified using a stream function. These equations are then transformed from non-linear partial differential equations (PDEs) into non-linear ordinary differential equations (ODEs) through similarity transformations. The resulting ordinary differential equations are solved numerically using the bvp4c method. Subsequently, the influence of various physical parameters on the velocity, temperature, and concentration profiles is analyzed. It is observed that the Casson fluid parameter enhances the velocity profile while slowing down the temperature and concentration profiles. Conversely, the Grashof number exhibits behavior opposite to that of the Casson fluid parameter. Furthermore, the variations of different parameters on the velocity, temperature, concentration, skin friction coefficient, temperature gradient, and Sherwood number are presented in both graphical and tabular forms. The numerical results are compared with existing literature Cortell (2007).

1. INTRODUCTION

One Due to wide selection of delicate applications of non-Newtonian fluid past a stretching sheet in many industries such as food processes, well water pollution, rock oil extraction, plastic material production, cooling of the nuclear reactors, industrialized of the electronic chips etc. Such kind of flows are encountered in extrusion processes such as fiber and wire drawing, hot rolling, crystal growing, glass fiber and paper production etc. One of the type of non-Newtonian fluid is Casson fluid which is by yield stress that is wide recycled for modeling blood movement in slender arteries at low shear amounts. Basically the Casson fluid model was initially established by Casson [1] for research of production of toners and semiconductor interruptions. Casson fluid partakes necessary uses in chemical compound manufacturing and also in biomechanics [2]. The major motivation came for the Casson fluid because the greatest physics model designed for blood and the chocolate [3-4]. On behalf of such applications, several scientists have thought-about Casson fluid used for various geometries. Shawky [5] investigated the heat and material transference appliances in MHD flow of the Casson fluid above on a linear stretching sheet soaked in an exceedingly pours medium. Mukhopadhyay [6] and also Medikare et al. [7] studied the heat transferal impact on Casson fluid over a nonlinear stretching sheet within the nonexistence and existence of the viscous dissipation. Mythili et al. [8] discussed the effect of chemical reaction on Casson fluid flow and the presence of thermal radiation on a vertical cone. The influence of force field and heat transfer flow of the Casson fluid from side to side a permeable moderate was conferred by Ullah et al [9]. Imtiaz et al [10] established the mixed convection Casson fluid flow through a linear stretching container crammed with the nanofluid and convective boundary conditions. Furthermore, many researchers [11-17] have investigated Casson fluid phenomena by considering different aspects of geometry.
The thermal and convections phenomenon within the flow over a stretching/shrinking surfaces are helpful to investigate the heat related issues. Such situations happen in an exceedingly variety of manufacturing, geology and the energy storage uses. For instance, in hypersonic expeditions, rocket return to the combustion slots, gas ventilated nuclear-powered devices and the power plants used for the inter-planetary flying. In nature maximum of the issues coping by flow concluded a

*Corresponding author. Email: nazimtufail@gmail.com

moving surface are established through the effort of the boundary and resilience impacts concluded with thermal and the concentration convections. Sensible samples of such flows are start essential receiver showing to wind tides, electrical strategies cool by fans, atomic containers cooled throughout alternative conclusion etc. K. Das [18] considered the slip effects on MHD mixed convection stagnation point flow of a micropolar fluid towards a shrinking vertical sheet. N. Kishan, and R. N. Srinivasmaripala [19] studied the MHD free convection flow past an infinite flat plate. Further, Z. Ismail and his coworkers [20] analyzed the unsteady boundary layer MHD free convection flow in a porous medium with constant mass diffusion and Newtonian heating. H. T. Alkasasbeh et al. [21] considered radiation effect on MHD free convection flow about a solid sphere and calculated numerical solutions. The effects of mixed convection on Casson fluid with mass transfer are evaluated by M. Z. Salleh et al. [22]. Furthermore, S. Pramanik [23] assumed Casson fluid flow and heat transfer in presence of thermal radiation found the impact on heat transfer phenomenan. M.V. Ramana and et al. [24] estimated the effect of natural convection on heat and mass transfer with thermal radiation and Hall current phenomenan. Optimization of circular wavy cavity filled by nanofluids under the natural convection heat transfer condition is considered by M. Hatami et al. [25]. Recently numerous other scientists [26-32] have attempted to explore the convection phenomena.

From aforementioned literature one can observe that very few efforts have been carried out for mixed convection with nanofluid effects. For that the Casson nanofluid over a stretching sheet is considered. The governing partial differential equations are converted into ordinary differential equations by suitable similarity transformations. The graphical results are plotted and numerical results are compared with [33]. Further, the main objective of this study is to measure the effects of Casson fluid parameter and Grashof number on velocity, temperature and concentration profiles. Furthermore, this model can be used for other geometries like nonlinear stretching sheet, shrinking sheet, slip condition, no slip condition etc.

2. MATHEMATICAL MODELLING

The unsteady non-Newtonian fluid flow called Casson fluid of material transfer and heat concluded on a stretched surface using permeable medium in the existence of the thermal radiation, uniform magnetic field, Joule heating property, mixed convection and viscous dissipation effects are considered. The flow is in Y>0 direction. The X and Y components along the stretched surface and upright to the surface in the order. Two forces which are equal but opposite applied in X-axis to preserve the exterior enlarge and origin fixed. The strength of magnetic field B_0 is applied to Y-axis which is represented if Fig. 1. Suppose little value of magnetic Reynolds number and the fluid is electrically leading to slight inflamed magnetic field. There is no electric field in this process

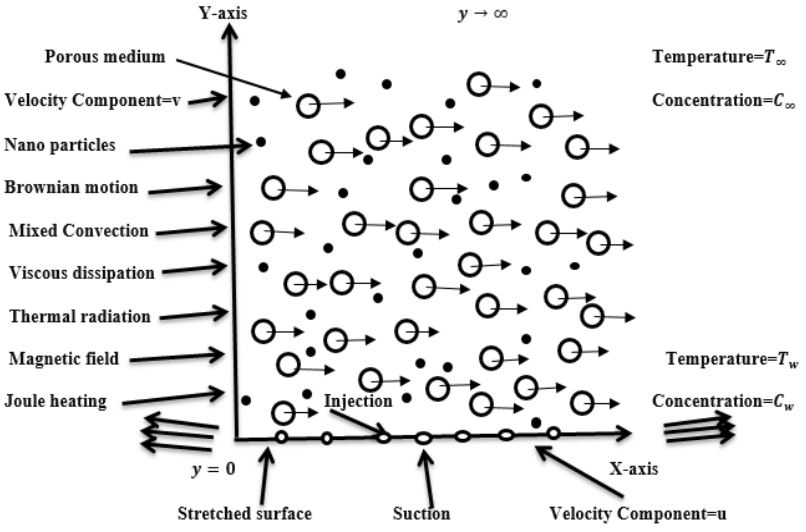

Fig. 1. Flow Diagram

After applying the assumptions on the law of conservation of mass, momentum, energy and on mass transfer equations [28] the following (1)-(4) equations are attained.

$$\frac{\partial u}{\partial x}+\frac{\partial v}{\partial y}=0, \tag{1}$$

$$\frac{\partial u}{\partial t}+u\frac{\partial u}{\partial x}+v\frac{\partial u}{\partial y}=\upsilon\left(1+\frac{1}{\beta}\right)\frac{\partial^2 u}{\partial y^2}-\frac{\delta B^2}{\rho}u+g\beta_1(T-T_\infty)+g\beta_2(C-C_\infty)-\frac{\nu}{k'}u\,, \tag{2}$$

$$\frac{\partial T}{\partial t}+ u\frac{\partial T}{\partial x}+v\frac{\partial T}{\partial y}=\frac{k}{\rho c_p}\frac{\partial^2 T}{\partial y^2}+\tau\left(D_B\frac{\partial C}{\partial y}\frac{\partial T}{\partial y}+\left(\frac{D_T}{T_\infty}\right)\left(\frac{\partial T}{\partial y}\right)^2\right)+\frac{\mu_B}{\rho C_p}\left(1+\frac{1}{\beta}\right)\left(\frac{\partial u}{\partial y}\right)^2+$$
$$\frac{\delta B^2}{\rho C_p}u^2+\frac{Q_0(T-T_\infty)}{\rho C_p}+\frac{16\delta_1 T_\infty^3}{3\rho C_p K_1}\frac{\partial^2 T}{\partial y^2}, \tag{3}$$

$$\frac{\partial C}{\partial t}+u\frac{\partial C}{\partial x}+v\frac{\partial C}{\partial y}=D_B\frac{\partial^2 C}{\partial y^2}+\left(\frac{D_T}{T_\infty}\right)\left(\frac{\partial^2 T}{\partial y^2}\right). \tag{4}$$

The boundary conditions [28] related to above described system are

$$u=u_w,\quad v=v_w,\quad T=T_w,\quad C=C_w \quad \text{at} \quad y=0,$$
$$u\to 0,\quad T=T_\infty,\quad C=C_\infty \quad \text{as} \quad y\to\infty. \tag{5}$$

$$u_w=\frac{ax}{1-\gamma t},\qquad v_w=-\sqrt{\frac{\nu u_w}{x}}f(0),\qquad T_w(x,t)=T_\infty+\frac{bx}{1-\gamma t},\ C_w(x,t)=C_\infty+\frac{cx}{1-\gamma t}. \tag{6}$$

Here c is greater than zero which is the enlarging constant, T_w represents the uniform wall temperature, T_∞ represents the temperature distant away from the surface, C_w represents the concentration at wall and C_∞ represents concentration at infinity. Here $B(t)=B_0(1-\gamma t)^{-1/2}$, B_0 denotes the uniform magnetic field strength, u and v are signifying the velocity components alongside x-axis and the y-axis in that order, $\beta=\frac{\mu_B\sqrt{2\pi_c}}{P_y}$ is the Casson fluid parameter, $\alpha=\frac{k}{(\rho c_P)_f}$ represent the thermal diffusivity of base fluid. Moreover $T, C, \rho, c_P, \sigma, \beta_1, \beta_2$ and k are local temperature, local nano particles volume, fraction fluid density, particular heat with constant pressure, the electrical conductivity of fluid, body forces and thermal conductivity respectively. Further $Q_0, \delta_1, K_1, k', D_T$ and D_B represents dimensionless source sink, mean absorption coefficient, Stefan Boltzmann constant, porous medium, thermophoretic diffusion coefficient and Brownian diffusion coefficient respectively. Also here $\nu=\frac{\mu}{\rho}$, where μ represents the fluid viscosity and ρ shows fluid density.

Now some dimensionless quantities are introduced which are subsequent transformations applied to transform the equations (1-4) to non-linear ODE's.

$$\eta=\sqrt{\frac{u_w}{\nu x}}y,\Psi=\sqrt{\nu x u_w}f(\eta),\theta(\eta)=\frac{T-T_\infty}{T_w-T_\infty},\ \phi(\eta)=\frac{C-C_\infty}{C_w-C_\infty}. \tag{7}$$

Where *Ψ(x, y)* is the stream function, the components of the velocity are $u=\frac{\partial\Psi}{\partial y}$ and $v=-\frac{\partial\Psi}{\partial x}$ and $\theta(\eta)$, $\phi(\eta)$ are non-dimensional temperature and concentration parameters respectively.

By applying the similarity transformation (7) on equation (1-4) the following system of ODE's appeared

$$\left(1+\tfrac{1}{\beta}\right)f'''+f'f''-f'^2-A\left(f'+\tfrac{1}{2}\eta f''\right)-Mf'+Gr\theta+Gc\phi-\tfrac{1}{K}f'=0, \tag{8}$$

$$\left(1+\frac{4}{3Nr}\right)\theta''+Pr[f\theta'-f'\theta]-PrA\left[\theta+\frac{1}{2}\eta\theta'\right]+PrEc\left(1+\frac{1}{\beta}\right)f''^2+MPrEcf'^2$$
$$+PrNt\theta'^2+PrNb\phi'\theta'+PrQ\theta=0, \tag{9}$$

$$\phi''+Le[f\phi'-f'\phi]-LeA\left[\phi+\tfrac{1}{2}\eta\phi'\right]+\frac{Nt}{Nb}\theta''=0. \tag{10}$$

The associated boundary condition (5), take the form after using (7) as

$$f'(0)=1,\qquad f(0)=S,\quad \theta(0)=1,\quad \phi(0)=1 \quad \text{at } \eta=0,$$
$$f'(\eta)\to 0,\quad \theta(\eta)\to 0,\quad \phi(\eta)\to 0 \quad as \quad \eta\to\infty. \tag{11}$$

Now the flow in the form of skin-friction c_f, heat transfer rate on Nusselt number Nu_x and concentration rate in term of Sherwood number Sh_x are given by

$$c_f=\frac{\tau_{wx}}{\rho u_w^2},\ Nu_x=\frac{q_w x}{k(T_w-T_\infty)},\qquad Sh_x=\frac{q_m x}{D_B(C_w-C_\infty)}. \tag{12}$$

Where C_f represents local skin friction, Nu_x is the local Nusselt number and Sh_x shows local Sherwood number.

Here τ_{wx}, q_w , q_m are shear stress, heat flux and mass flux respectively and specified by

$$\tau_{wx}=\left(\mu_B+\frac{\rho_y}{\sqrt{2\pi_c}}\right)\left(\frac{\partial u}{\partial y}\right)_{y=0},\ q_w=-[k+\tfrac{16\delta_1 T_\infty^3}{3K_1}](\frac{\partial T}{\partial y})_{y=0},\qquad q_m=-D_B\left(\frac{\partial C}{\partial y}\right)_{y=0}. \tag{13}$$

Now using transformation (7) on (13) and the dimensionless form of C_f, Nu_x and Sh_x are $Re_x^{1/2}C_f=\left(1+\frac{1}{\beta}\right)f''(0)$,

$$Re_x^{1/2} Nu_x = -[1 + \frac{4}{3Nr}]\theta'(0), \quad Re_x^{1/2} Sh_x = -\phi'(0). \tag{14}$$

Where $M^2 = \frac{\sigma B_0^2}{\rho a}$ is the parameter of the magnetic field, $A = \frac{\gamma}{a}$ represents unsteadiness parameter, S denotes the suction/injection parameter with S greater than zero for suction and less than zero for injection, $Pr = \frac{\mu c_p}{k}$ represents the Prandtl number and $Ec = \frac{U_w^2}{c_p(T_w - T_\infty)}$ is denoted as Eckert number. Further, $Nr = \frac{kK_1}{4\delta_1 T_\infty^3}$, $Nt = \frac{\tau D_T (T_w - T_\infty)}{\nu T_\infty}$, $Nb = \frac{\tau D_B (C_w - C_\infty)}{\vartheta}$, $Q = \frac{Q_0(1-\gamma t)}{a\rho c_p}$, $\frac{1}{K} = \frac{\nu}{k'a}(1 - \gamma t)$, represents radiation, thermophoretic, Brownian, source/sink and porosity parameter. Similarly $Le = \frac{\nu}{D_B}$, $Gr = g\beta_1 bx(1 - \gamma t)$, $Gc = g\beta_2 cx(1 - \gamma t)$ Lewis number, Grashof number and modified Grashof number respectively and $Re_x = \frac{u_w x}{\nu}$ represents by local Reynolds number.

3. RESULTS AND DISCUSSION

By closely observing the nature of the problem as depicted by the set of highly nonlinear ordinary differential equations (8-10) and boundary conditions (11), the bvp4c code is applied to solve the problem. The effects of various pertinent parameters involving in the considered problem on flow $f'(\eta)$, thermal $\theta(\eta)$ and nanoparticles concentration $\phi(\eta)$ characteristics are presented through graphs and tables.

The Figs 2-4 displayed the impacts of A on the $f'(\eta)$, $\theta(\eta)$ and $\phi(\eta)$. It is seen in the Fig. 2, Fig. 3 and Fig.4 that the flow, thermal and concentration profile decreases due to increase of unsteady parameter$A$. Figs 5-7 depicts the influence of Casson fluid parameter β on the $f'(\eta)$, $\theta(\eta)$ and $\phi(\eta)$ respectively. Figs 5-6 displays with the increment in the value of β the $f'(\eta)$ and $\theta(\eta)$ decreases. In fact the yield stress decreases which suppresses the fluid velocity. It is noticed from Fig. 7 that the $\phi(\eta)$ increases due to increase in β. The impacts of Ec on the $\theta(\eta)$ is depicted in Fig. 8. It is observed that $\theta(\eta)$ enhances due to the increase in the Ec number. Figs 9-10 shows the increment in the value of Gc the flow profile $f'(\eta)$ increases but $\theta(\eta)$ decreases. Fig.11-12 shows the increment in $f'(\eta)$ and $\theta(\eta)$ when increase the value of Gr. It is shown in Fig. 13 that the $f'(\eta)$ rises with the value of K. Due to the drag force K resists but it appears as denominator in the modeling so as a result it rises the fluid velocity. It is displayed in Fig. 14 that the $\phi(\eta)$ declines with the increase in Le. Further, Fig. 15 and Fig. 16 represents the impact of M on the $f'(\eta)$ and $\phi(\eta)$. Therefore as M increases, so does the $f'(\eta)$ and $\phi(\eta)$ decreases. It is the fact that the Lorentz force (resistive force) reduced the primary flow. It is observed in the Fig. 17 that, as the value of M increase the $\theta(\eta)$ also increases. Actually the Lorentz force increases the temperature of the particles and the transport of heat increases when the magnetic field parameter increases. In Figs 18-19 represents $\theta(\eta)$ and $\phi(\eta)$ are both increases with increasing values of Nb. This is due to the fact that the Brownian motion of nanoparticles increases the heat transport phenomenon. It is experiences in the Fig. 20 that $\theta(\eta)$ increases with increasing values of Nr. It is presented in Fig. 21 that the $\theta(\eta)$ increases with the rise of Nt. Thus the presence of thermophoretic force has a significant effect on heat to boast it. It is observed from Fig. 22 that as the value of Nt increases, the $\phi(\eta)$ is decreases. Furthermore, Figs 23-24 clarifies that the dimensionless $\theta(\eta)$ and $\phi(\eta)$ for changed values of the Pr. It is observed from Figs 23-24 that increase in Pr leads to increase in $\theta(\eta)$ but $\phi(\eta)$ decreases. The influence of Q on the $\theta(\eta)$ is clearly observed in Fig. 25. The Fig. 25 shows with the increase in the value of Q the $\theta(\eta)$ increases. It is revealed in Fig. 26 that the $f'(\eta)$ increases with the increase of S.

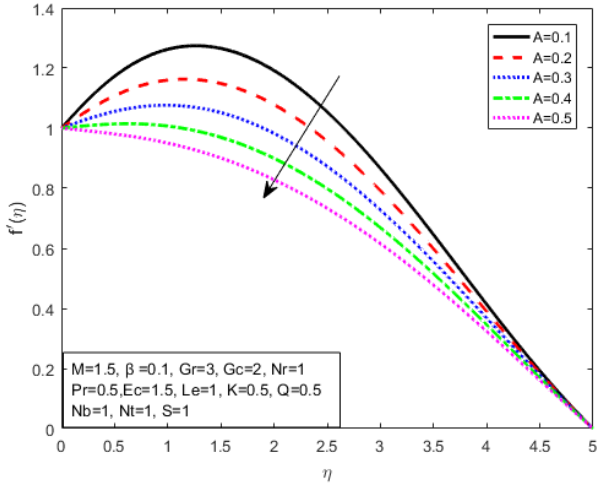

Fig. 2. Influence of A on $f'(\eta)$

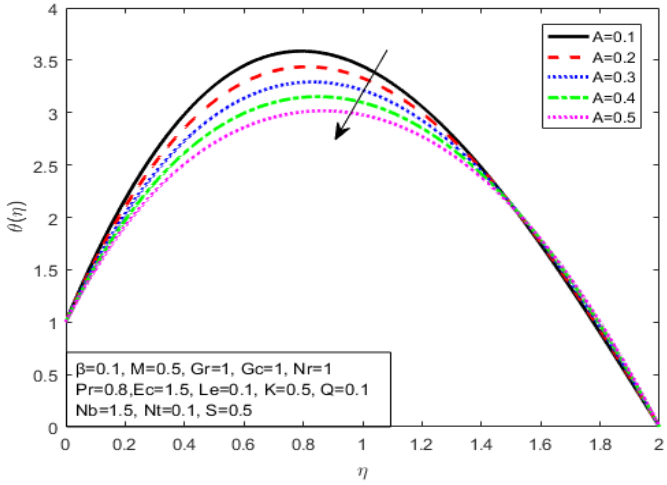

Fig. 3. Influence of A on $\theta(\eta)$

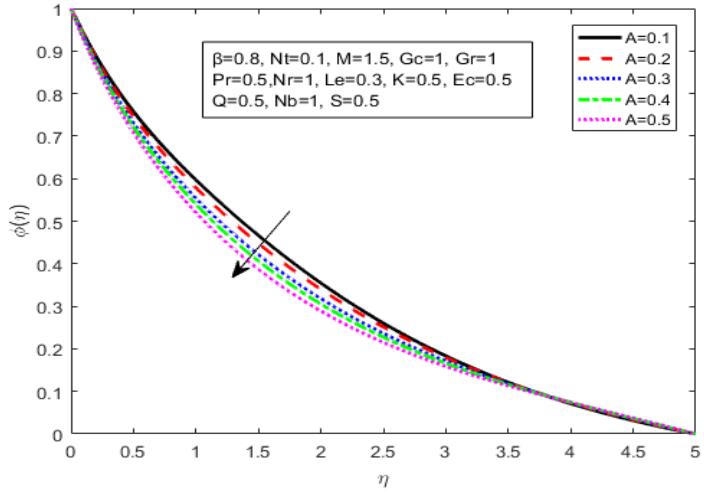

Fig. 4. Influence of A on $\phi(\eta)$

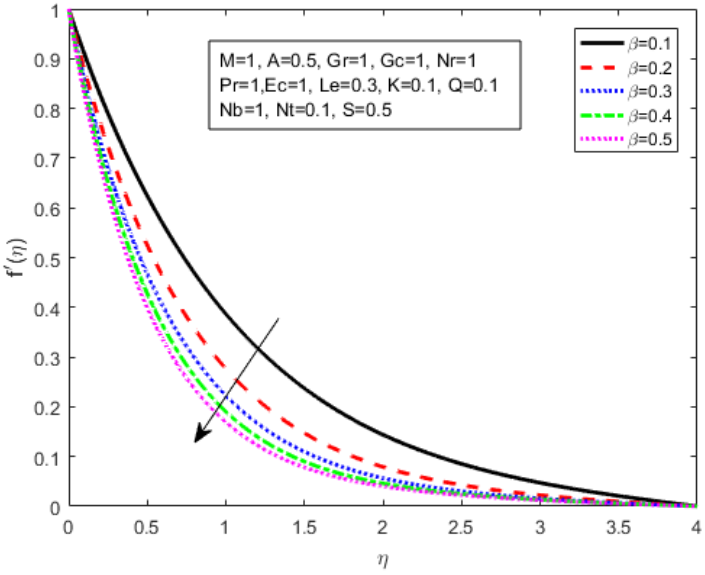

Fig. 5. Influence of β on $f'(\eta)$

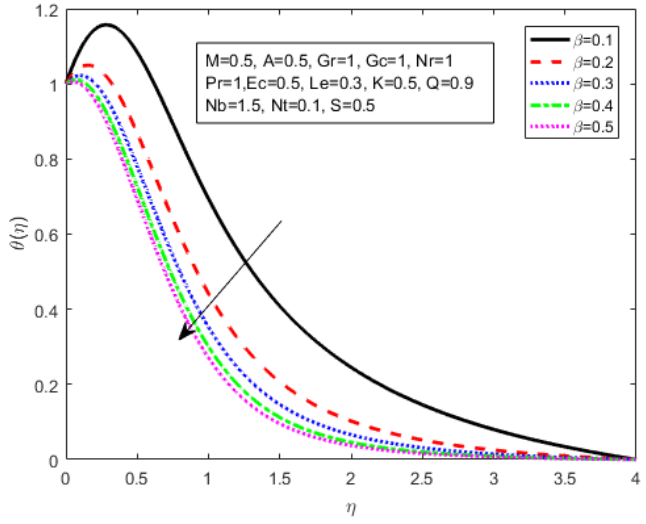

Fig. 6. Influence of βon $\theta(\eta)$

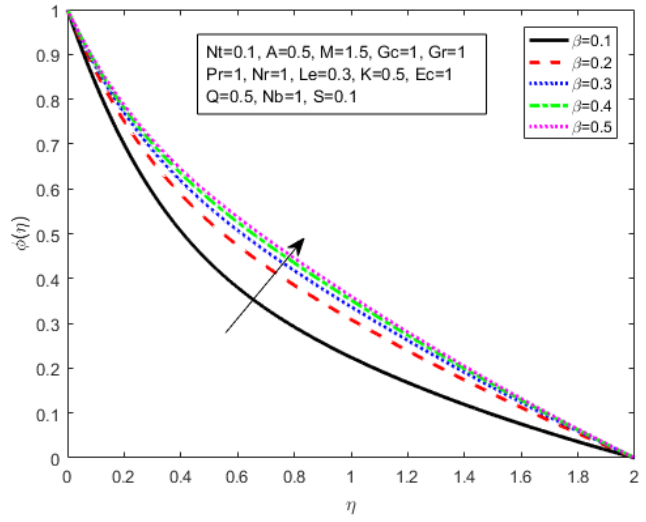

Fig. 7. Influence of β on $\phi(\eta)$

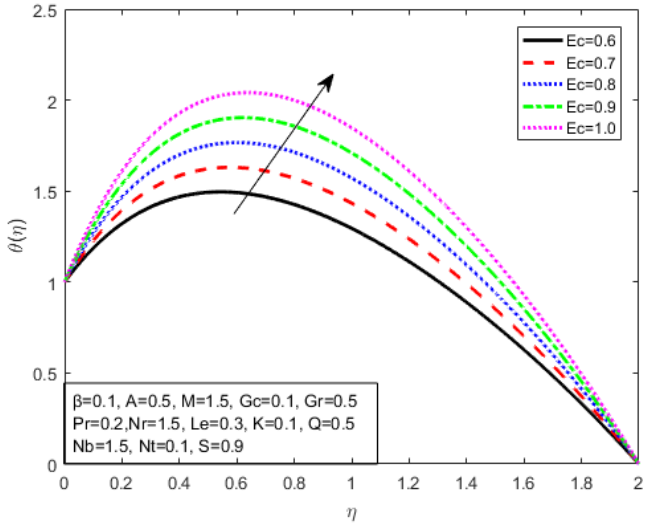

Fig. 8. Influence of *Ec* on $\theta(\eta)$

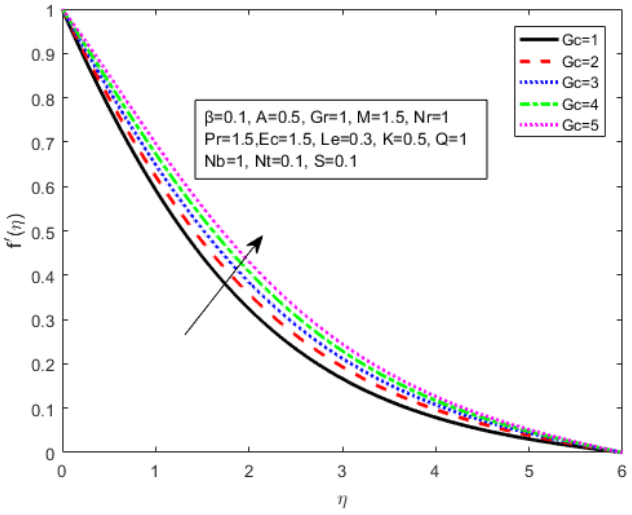

Fig. 9. Influence of Gc on $f'(\eta)$

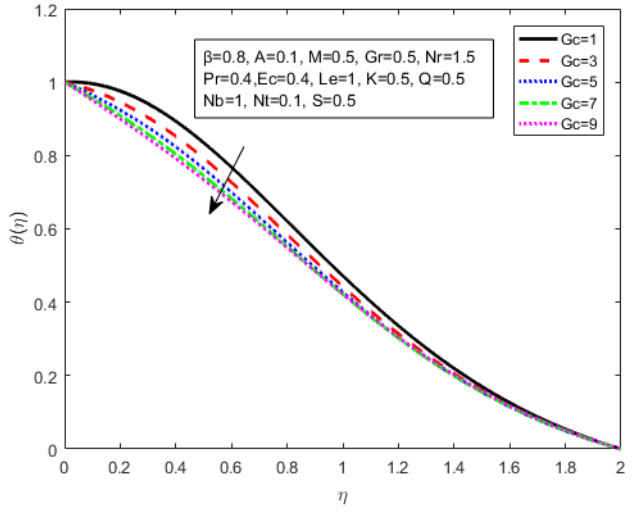

Fig. 10. Influence of Gc on $\theta(\eta)$

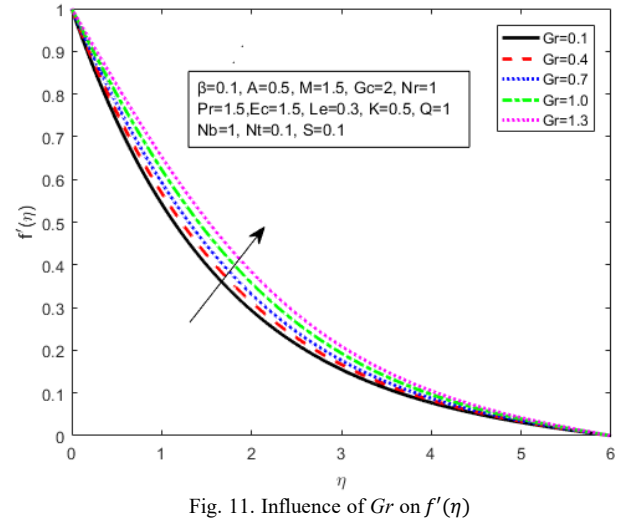

Fig. 11. Influence of Gr on $f'(\eta)$

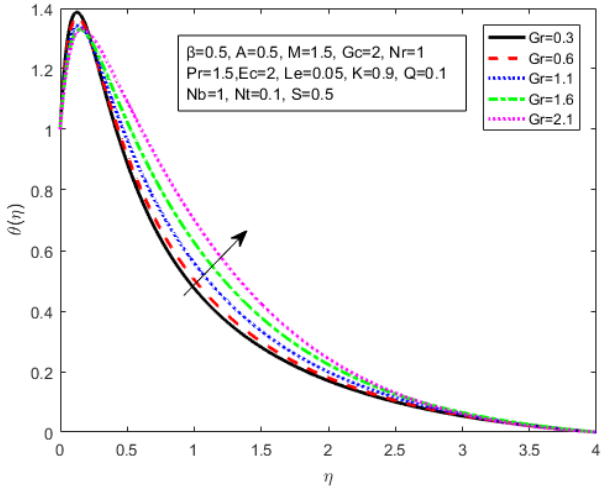

Fig. 12. Influence of Gr on $\theta(\eta)$

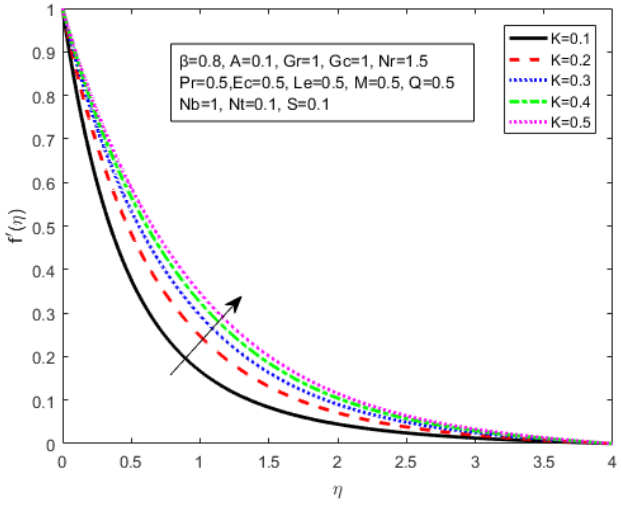

Fig. 13. Influence of K on $f'(\eta)$

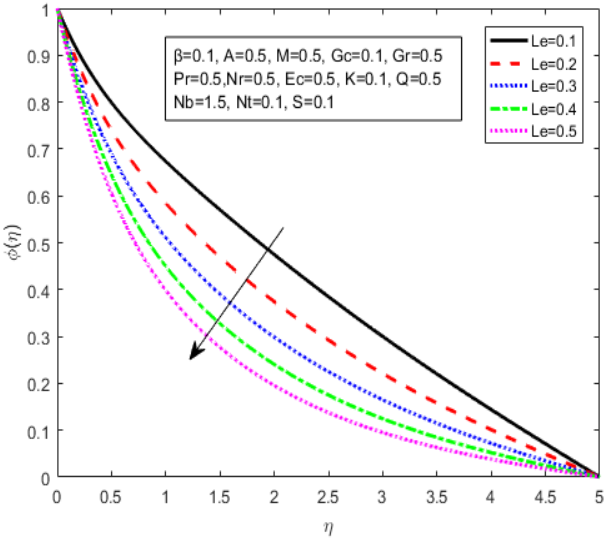

Fig. 14. Influence of Le on $\phi(\eta)$

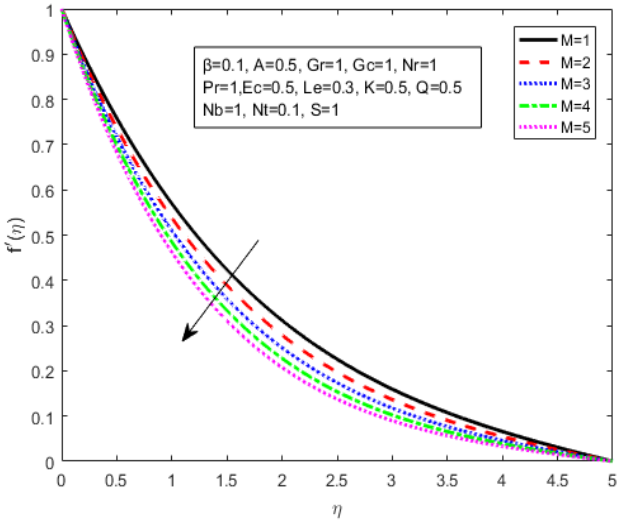

Fig. 15. Influence of M on $f'(\eta)$

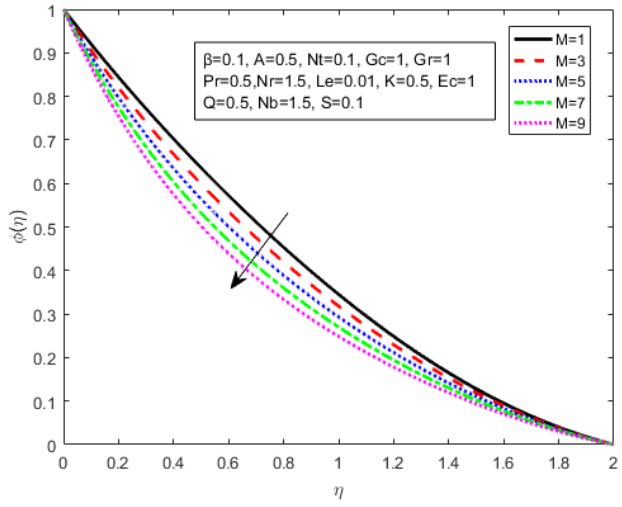

Fig. 16. Influence of M on $\phi(\eta)$

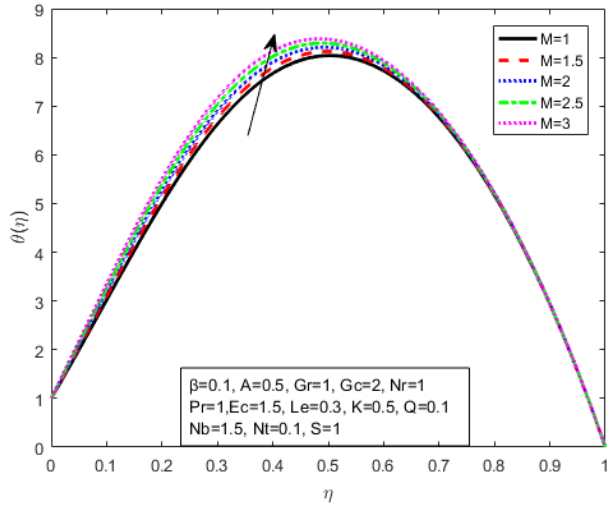

Fig. 17. Influence of M on $\theta(\eta)$

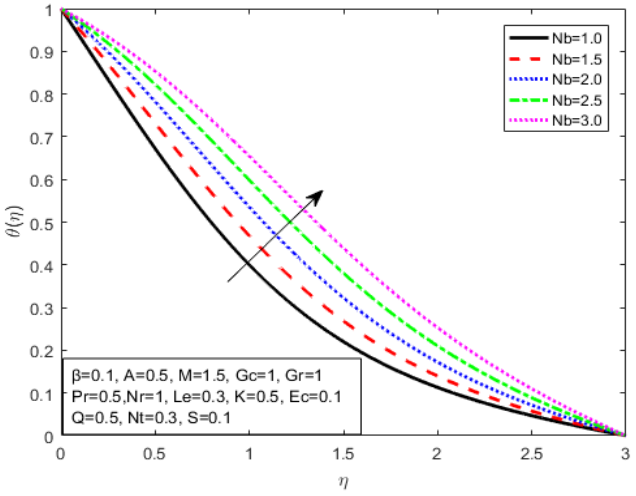

Fig. 18. Influence of *Nb* on $\theta(\eta)$

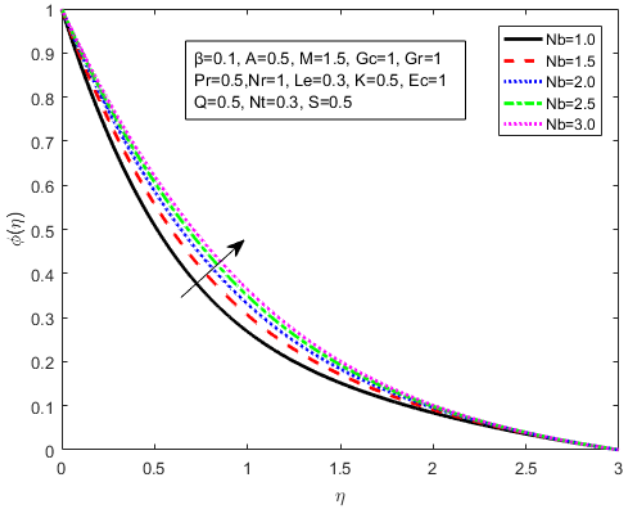

Fig. 19. Influence of *Nb* on $\phi(\eta)$

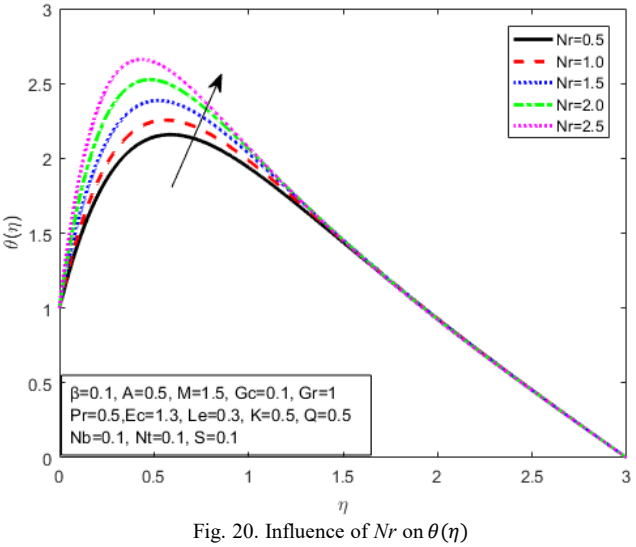

Fig. 20. Influence of *Nr* on $\theta(\eta)$

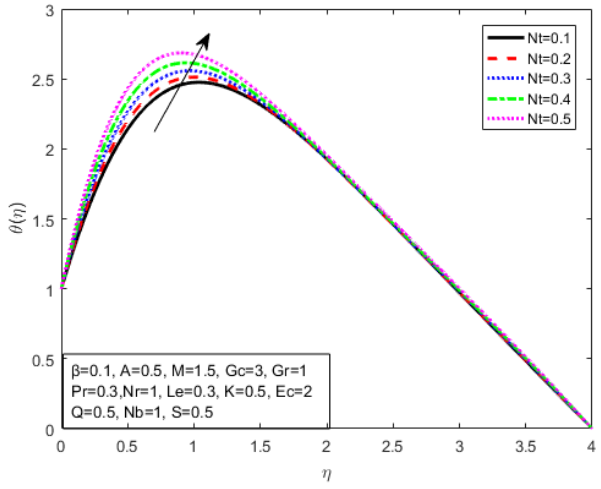

Fig. 21. Influence of *Nt* on $\theta(\eta)$

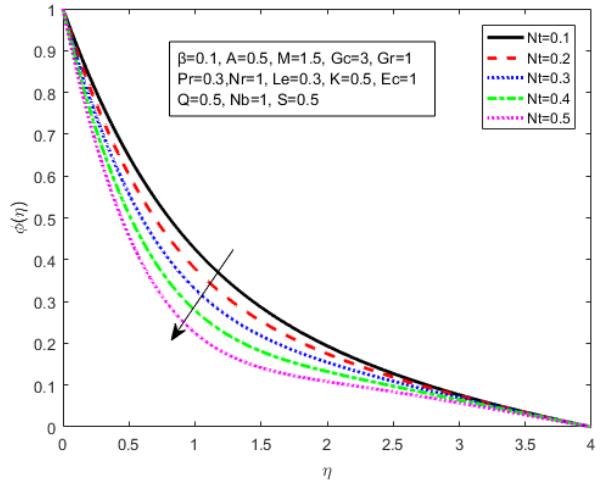

Fig. 22. Influence of *Nt* on $\phi(\eta)$

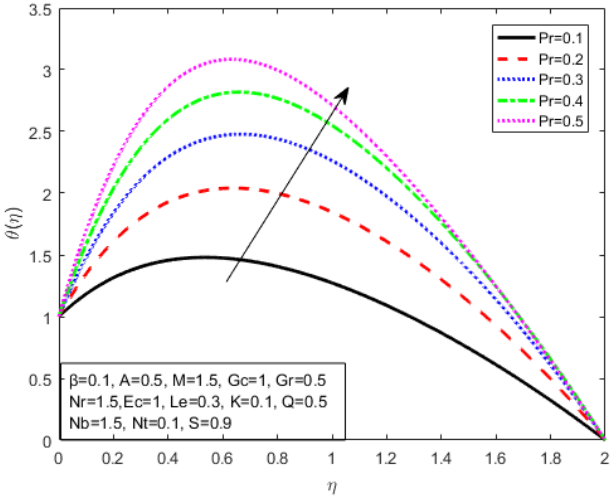

Fig. 23. Influence of *Pr* on $\theta(\eta)$

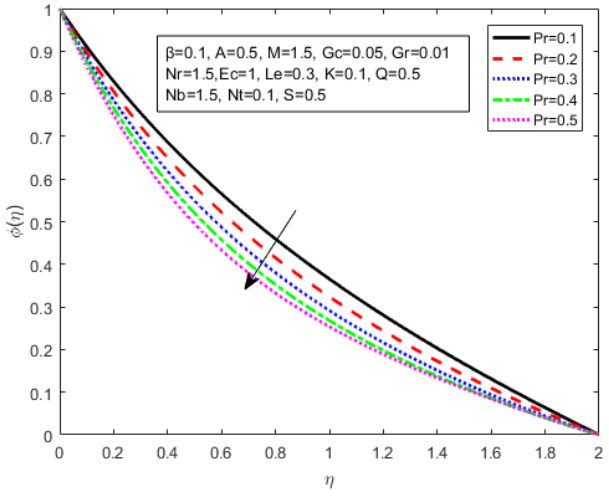

Fig. 24. Influence of Pr on $\phi(\eta)$

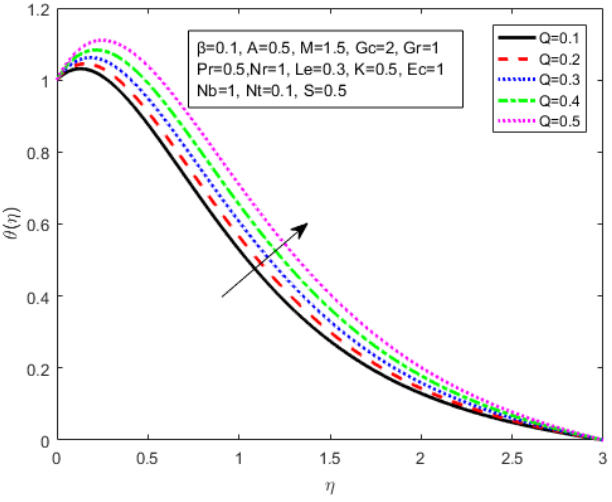

Fig. 25. Influence of Q on $\theta(\eta)$

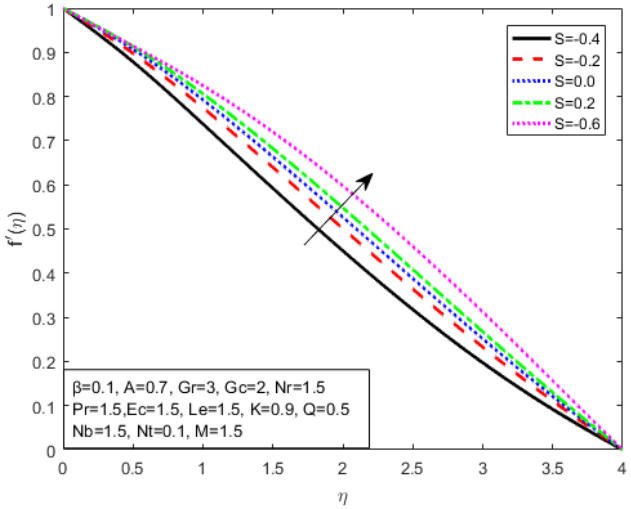

Fig. 26. Influence of S on $f'(\eta)$

The values of local skin-friction coefficient, the local Nusselt number and local Sherwood numbers are tabulated in Table 1, Table 2 and Table 3 respectively.

It is noted that from Table 1, the $\left(\mathbf{1}+\frac{\mathbf{1}}{\boldsymbol{\beta}}\right)f''(0)$ enhances with increasing in magnetic field *M*, unsteadiness parameter *A*, suction/injection parameter *S* whereas declines with increasing in Casson fluid parameter β, Grashof number *Gr*, modified Grashof number *Gc*, porous medium *K*.

Further, it is also pointed in Table 2 that the $-\theta'(0)$ goes up with increasing in Eckert number *Ec*, thermophoretic number *Nt*, radiation parameter Nr and source/sink parameter Q whereas declines with increasing in Casson fluid parameter β, unsteadiness parameter *A*, Brownian parameter *Nb*, Grashof number *Gr*, modified Grashof number *Gc* and porous medium *K*.

Furthermore, it is also observed from the Table 3 that the $-\phi'(0)$ declines with increasing in Casson fluid parameter β, unsteadiness parameter *A*, Brownian parameter *Nb*, Grashof number *Gr*, modified Grashof number *Gc* and porous medium *K*. Although increments with increasing in Eckert number *Ec*, thermophoretic number *Nt*, radiation parameter *Nr*, source/sink parameter *Q*, Lewis number *Le*.

TABLE I. VARIATIONS OF $\left(1+\frac{1}{\beta}\right)f''(0)$ BY CHANGING DIFFERENT PARAMETERS

$\boldsymbol{\beta}$	$\boldsymbol{M}$	$\boldsymbol{A}$	$\boldsymbol{S}$	$\boldsymbol{Gr}$	$\boldsymbol{Gc}$	$\boldsymbol{K}$	$\left(\mathbf{1}+\frac{\mathbf{1}}{\boldsymbol{\beta}}\right)f''(\mathbf{0})$
0.1	1.0	1.0	1.0	1.0	1.0	0.5	6.04741
0.2							4.48942
0.5							3.20726
0.8							2.79758
0.1	0.0	1.0	1.0	1.0	1.0	0.5	5.30214
	0.5						5.68156
	1.0						6.04741
	1.5						6.40091
0.1	1.0	0.0	1.0	1.0	1.0	0.5	4.96485
		0.2					5.20061
		0.4					5.42851
		0.6					5.64642
0.1	1.0	1.0	1.0	1.0	1.0	0.5	6.04741
			1.5				6.39982
			2.0				6.76419
			2.5				7.13755
0.1	1.0	1.0	1.0	0.5	1.0	0.5	6.71632
				1.5			5.42036
				2.5			4.23248
				3.5			3.07529
0.1	1.0	1.0	1.0	1.0	0.5	0.5	6.20297
					1.0		6.04741
					1.5		5.89162
					2.0		5.73562
0.1	1.0	1.0	1.0	1.0	1.0	0.5	6.04741
						1.5	4.86077
						2.5	4.59764
						3.5	4.48164

TABLE II. VARIATIONS OF $-\theta'(0)$ BY CHANGING DIFFERENT PARAMETERS

$\boldsymbol{\beta}$	$\boldsymbol{A}$	$\boldsymbol{Ec}$	$\boldsymbol{Nt}$	$\boldsymbol{Nb}$	$\boldsymbol{Nr}$	$\boldsymbol{Q}$	$\boldsymbol{Gr}$	$\boldsymbol{Gc}$	$\boldsymbol{K}$	$-\boldsymbol{\theta}'(\mathbf{0})$
0.1	1.0	1.0	1.0	1.0	1.0	1.0	1.0	1.0	0.5	0.518857
0.2										0.296054
0.5										0.124975
0.8										0.069751
0.1	0.0	1.0	1.0	1.0	1.0	1.0	1.0	1.0	0.5	1.783781
	0.2									1.474262
	0.4									1.217911
	0.6									1.005180
0.1	1.0	0.6	1.0	1.0	1.0	1.0	1.0	1.0	0.5	0.086855
		0.7								0.195153
		0.8								0.303246
		0.9								0.411144
0.1	1.0	1.0	0.0	1.0	1.0	1.0	1.0	1.0	0.5	0.475777

			0.2							0.483777
			0.4							0.492045
			0.6							5.006281
0.1	1.0	1.0	1.0	1.0	1.0	1.0	1.0	1.0	0.5	0.518857
				1.5						0.487708
				2.0						0.459847
				2.5						0.433842
0.1	1.0	1.0	1.0	1.0	0.5	1.0	1.0	1.0	0.5	0.277629
					1.0					0.518857
					1.5					0.660154
					2.0					0.753601
0.1	1.0	1.0	1.0	1.0	1.0	0.0	1.0	1.0	0.5	0.112093
						0.3				0.213072
						0.5				0.288261
						0.8				0.417432
0.1	1.0	1.0	1.0	1.0	1.0	1.0	0.5	1.0	0.5	0.641639
							1.5			0.414004
							2.5			0.244912
							3.5			0.118250
0.1	1.0	1.0	1.0	1.0	1.0	1.0	1.0	0.5	0.5	0.527636
								1.0		0.518857
								1.5		0.510363
								2.0		0.502153
0.1	1.0	1.0	1.0	1.0	1.0	1.0	1.0	1.0	0.5	0.518857
									1.5	0.359644
									2.5	0.328198
									3.5	0.314804

TABLE III. VARIATIONS OF $-\phi'(0)$ BY CHANGING DIFFERENT PARAMETERS

β	A	Ec	Nt	Nb	Nr	Q	Le	Gr	Gc	K	$-\phi'(0)$
0.1	1.0	1.0	1.0	1.0	1.0	1.0	1.0	1.0	1.0	0.5	2.75385
0.2											2.52679
0.5											2.34636
0.8											2.28279
0.1	0.0	1.0	1.0	1.0	1.0	1.0	1.0	1.0	1.0	0.5	2.98507
	0.2										2.92032
	0.4										2.86565
	0.6										2.82015
0.1	1.0	0.5	1.0	1.0	1.0	1.0	1.0	1.0	1.0	0.5	2.28995
		1.0									2.75385
		1.5									3.22221
		2.0									3.69679
0.1	1.0	1.0	0.0	1.0	1.0	1.0	1.0	1.0	1.0	0.5	2.01714
			0.2								2.15779
			0.4						.		2.30155
			0.6								2.44863
0.1	1.0	1.0	1.0	1.0	1.0	1.0	1.0	1.0	1.0	0.5	2.75385
				1.5							2.48395
				2.0							2.35144
				2.5							2.27298
0.1	1.0	1.0	1.0	1.0	0.5	1.0	1.0	1.0	1.0	0.5	2.51616
					1.0						2.75385
					1.5						2.89559
					2.0						2.99051
0.1	1.0	1.0	1.0	1.0	1.0	0.4	1.0	1.0	1.0	0.5	2.56891
						0.5					2.59673
						0.6					2.62560
						0.7					2.65562
0.1	1.0	1.0	1.0	1.0	1.0	1.0	0.2	1.0	1.0	0.5	1.62981
							0.4				1.93972
							0.6				2.22539
							0.8				2.49517
0.1	1.0	1.0	1.0	1.0	1.0	1.0	1.0	0.5	1.0	0.5	2.83825
								1.5			2.67906
								2.5			2.55354

								3.5			2.45509
0.1	1.0	1.0	1.0	1.0	1.0	1.0	1.0	1.0	0.5	0.5	2.75848
									1.0		2.75385
									1.5		2.74945
									2.0		2.74527
0.1	1.0	1.0	1.0	1.0	1.0	1.0	1.0	1.0	1.0	0.5	2.75385
										1.5	2.64272
										2.5	2.62106
										3.5	2.61185

In Table 4, the comparison is presented of skin friction profile $f''(0)$ with the Cortell [33] by setting A=0, S=0, $\frac{1}{\beta}=\frac{1}{K}=0$, Gc=0, Gr=0 and M=0. It is observed that our results appears with good agreement with those reported earlier.

TABLE IV. COMPARISON OF SKIN FRICTION WITH CARTELL[33]

M	$\lvert f''(0)\rvert$**[33]**	$\lvert f''(0)\rvert$**Present**
0.0	1	1.0000
0.2	1.09545	1.09555
0.5	1.22474	1.22485
1.0	1.4142136	1.41421
1.2	1.48324	1.48320
1.5	1.58114	1.58110
2.0	1.7320508	1.732060

4. CONCLUSION

The present research is on an unstable nanofluid flow of Casson with mixed convection, Joule heating, and effects of mass transfer over stretching surface that is a numerical analysis. In this analysis the transformed ODE's were solved numerically using the method bvp4c. From this study initiate the following results. The numerical results attained very well with previously published data for some particular cases of the present study. From the present study following observations are found.

- The velocity of fluid f' increments with the increasing *Gr, Gc, K, S* whereas it declines with increasing in *A,* β, *M.*
- The temperature profile θ increments with the increasing in *Ec, Gr, M, Nb, Nr, Nt, Pr, Q* whereas it declines with increasing in *A,* β, *Gc, K*.
- The concentration profile ϕ declines with the increasing in *A, Ec, Gr, K, Le, M, Nt, Pr,* whereas it increments with increasing in β, *Nb, Nr*.
- The skin friction coefficient $\left(\mathbf{1}+\frac{\mathbf{1}}{\boldsymbol{\beta}}\right)f''(0)$ increments with increasing in *M, A, S* whereas declines with increasing in β, *Gr, Gc, K*.
- The local Nusselt number $-\theta'(0)$ increments with increasing in *Ec, Nt, Nr* and *Q* whereas declines with increasing in β, *A, Nb, Gr, Gc* and *K*.
- The local Sherwood Number $-\phi'(0)$ declines with increasing in β, *A, Nb, Gr, Gc* and *K*. whereas increments with increasing in *Ec, Nt, Nr, Q, Le.*

Conflicts Of Interest

The author's paper explicitly states that there are no conflicts of interest to be disclosed.

Funding

The author's paper clearly indicates that the research was conducted without any funding from external sources.

Acknowledgment

The author acknowledges the institution for their commitment to fostering a research-oriented culture and providing a platform for knowledge dissemination.

References

[1] N. Casson, (1959), A flow equation for pigment-oil suspensions of the printing ink type. In: Mill, C.C., Ed.

[2] P. S. Gupta and A. S. Gupta, (1977), Heat and mass transfer on a stretching sheet with suction and blowing, Can. J. Chem. Eng. 55, 744–746.

[3] M. Mustafa, T. Hayat, I. Pop and A. Aziz, (2011), Unsteady boundary layer flow of a Casson fluid due to an impulsively started moving flat plate, Journal of Heat Transfer-Asian Research, 40, 563- 576.

[4] S. Singh, (2011), Clinical significance of aspirin on blood flow through stenosis blood vessels, Journal of Biomimetics, Biomaterials and Tissue, 10, 17–24.

[5] H. M Shawky, (2012), Magnetohydrodynamic Casson fluid flow with heat and mass transfer through a porous medium over a stretching sheet, J. Porous Media, 15, 393–401.

[6] S. Mukhopadhyay, K. Bhattacharyya and T. Hayat, (2011), Exact solutions for the flow of Casson fluid over a stretching surface with transpiration and heat transfer effects, J. Chinese Physics B, 22, 114-¬701.

[7] M. Medikare, S. Joga and K. K Chidem, (2016), MHD stagnation point flow of a Casson fluid over a nonlinearly stretching sheet with viscous dissipation, Journal of Computational Mathematics, 37–48.

[8] D. Mythili and R. Sivaraj, (2016), Influence of higher order chemical reaction and non-uniform heat source/sink on Casson fluid flow over a vertical cone and flat plate, J. Molecular Solutes in ionic Liquids, 216, 466–475.

[9] I. Ullah, I. Khan and S. Shafie, (2016). Hydromagnetic Falkner-Skan flow of Casson fluid past a moving wedge with heat transfer, J. Alexendria Engineering, 55, 2139-2148.

[10] M. Imtiaz, T. Hayat and A. Alsaedi, (2016), Mixed convection flow of Casson nanofluid over a stretching cylinder with convective boundary conditions, J. Advanced Powder Technology, 27, 2245–2256.

[11] M. N. Tufail, A. Saeed Butt and A. Ali, (2016), Group theoretical analysis of non-Newtonian fluid flow of heat and mass transfer over a stretching surface in the presence of thermal radiation, JAFM, 9(3), 1515-1524.

[12] M.I. Khan, M. Waqas, T. Hayat, and A. Alsaedi, (2017). A comparative study of Casson fluid with homogeneous-heterogeneous reactions. Journal of Colloid and Interface Science, 498, 85-90.

[13] M. Tamoor, M.I. Waqas Khan, A. Alsaedi, and T. Hayat, (2017), Magnetohydrodynamic flow of Casson fluid over a stretching cylinder. Results in Physics, 7, 498-502.

[14] G. K. Ramesh, B. J. Gireesha, S. A. Shehzad and F. M. Abbasi, (2017), Analysis of heat transfer phenomenon in magnetohydrodynamic Casson fluid flow through Cattaneo–Christov heat diffusion theory, Communications in Theoretical Physics 68 (1), 91.

[15] G.T. Thammanna, K. Ganesh Kumar, B.J. Gireesha, G.K. Ramesh, and B.C. Prasannakumara (2017), Three dimensional MHD flow of couple stress Casson fluid past an unsteady stretching surface with chemical reaction, Results in Physics, 7, 4104-4110.

[16] M. Hamid, M. Usman, Z. Khan, R. Ahmad, and W. Wang, (2019), Dual solutions and stability analysis of flow and heat transfer of Casson fluid over a stretching sheet. Physics Letters A, 383(20), 2400-2408.

[17] V.K. Verma and S. Mondal, (2021), A brief review of numerical methods for heat and mass transfer of Casson fluids. Partial Differential Equations in Applied Mathematics, 3, 100034.

[18] K. Das, (2012). Slip effects on MHD mixed convection stagnation point flow of a micropolar fluid towards a shrinking vertical sheet, Comput. Math. Appl. 63, 255-267.

[19] N. Kishan, and R. N. Srinivasmaripala, (2013), MHD free convection flow past an infinite flat plate, ASME, Journal of Heat and Mass Transfer, 119, 89-96.

[20] Z. Ismail, I. Khan, A. G. Hussein and S. Shafie, (2014). Unsteady boundary layer MHD free convection flow in a porous medium with constant mass diffusion and Newtonian heating, The European Physical Journal Plus, 129, 1-46.

[21] H. T. Alkasasbeh, M.Z. Salleh, R. Nazar, and I. Pop, (2014). Numerical solutions of radiation effect on MHD free convection boundary layer flow about a solid sphere with Newtonian heating, J. Applied Mathematical Sciences, 8, 6989-7000.

[22] M. Z. Salleh, R. M. Tahar and I. Khan, (2014). Research on the Casson fluid with mass transfer and mixed convection, J. Neural Computing and Applications, 9, 456-650.

[23] S. Pramanik, (2014). Casson fluids flow and heat transfer past an exponentially porous stretching surface in presence of thermal radiation, Ain Shams Engineering Journal, 5, 205-212.

[24] M.V. Ramana Murthy, R. S. Raju and J. Anand Rao, (2015). Heat and Mass transfer effects on MHD natural

convection past an infinite vertical porous plate with thermal radiation and Hall current, Procedia Engineering Journal, 127, 1330-1337.

[25] M. Hatami, D. Song and D. Jing, (2016). Optimization of circular wavy cavity filled by nanofluids under the natural convection heat transfer condition, International Journal of Heat and Mass Transfer, 98, 758-767.

[26] A.K. Kareem and S. Gao,(2017). Mixed convection heat transfer of turbulent flow in a three-dimensional lid-driven cavity with a rotating cylinder. International Journal of Heat and Mass Transfer, 112, 185-200.

[27] A. S. Butt, A. Ali, M. N. Tufail, and Ahmer Mehmood, (2019), Theoretical Investigation of Entropy Generation Effects in Magnetohydrodynamic Flow of Casson Nanofluid Over an Unsteady Permeable Stretching Surface, Journal of Nanofluids, 8(1), 1-14.

[28] S. Yousefzadeh, H. Rajabi and N. Ghajari, (2020). Numerical investigation of mixed convection heat transfer behavior of nanofluid in a cavity with different heat transfer areas. J Therm Anal Calorim 140, 2779–2803.

[29] M. Ghaneifar, A. Raisi, and H.M. Ali, (2021), Mixed convection heat transfer of AL2O3 nanofluid in a horizontal channel subjected with two heat sources. J Therm Anal Calorim 143, 2761–2774.

[30] B. P. Geridonmez and H. F. Oztop, (2021), Mixed convection heat transfer in a lid-driven cavity under the effect of a partial magnetic field, Heat Transfer Engineering, 42:10, 875-887.

[31] Y.D. Reddy and I. Mangamma,(2023), Significance of radiation and chemical reaction on MHD heat transfer nanofluid flow over a nonlinearly porous stretching sheet with nonuniform heat source. Numerical Heat Transfer, Part A: Applications, 85(18), 2940–2966.

[32] S. Ashraf, M. Mushtaq, K. Jabeen, S. Farid and RMA Muntazir (2023), Heat and mass transfer of unsteady mixed convection flow of Casson fluid within the porous media under the influence of magnetic field over a nonlinear stretching sheet. Proceedings of the Institution of Mechanical Engineers, Part C: Journal of Mechanical Engineering Science, 237(1):20-38.

[33] R. Cortell, (2007). Viscous flow and heat transfer over a nonlinearly stretching sheet, Appl. Math. Computation, 184, 864–873.